

# New nitinol endovascular stent-graft system for abdominal aortic aneurysm with finite element analysis and experimental verification

Xiao-Chen Zhou, Fan Yang, Xiao-Yan Gong, Ming Zhao, Yu-Feng Zheng\*, Zhi-Li Sun\*

Received: 31 December 2018/Revised: 18 January 2019/Accepted: 14 March 2019
© The Nonferrous Metals Society of China and Springer-Verlag GmbH Germany, part of Springer Nature 2019

Abstract Abdominal aortic aneurysm (AAA) is one of the most common and catastrophic manifestations of the acute aortic syndrome that can be treated with endovascular aneurysm repair (EVAR) which requires a specially designed stent-graft system. In this work, a self-expanding nickel-titanium (nitinol) stent-graft system is aiming at AAA using finite element analysis (FEA) methods to analyze both fatigue behaviors and radial forces. Based on the systematic analysis of the parametric variations, a final stent-graft system was developed by the selection and arrangement of the individual stent components, targeting an optimal performance for the treatment of AAA. Experimental tests, animal tests and clinical trials were carried out to confirm the results. Both animal trials and clinical trials showed comparable curative effects with Medtronic Endurant stent-graft (SG) systems.

X.-C. Zhou, Y.-F. Zheng\*

Department of Materials Science and Engineering, College of Engineering, Peking University, Beijing 100871, China e-mail: yfzheng@pku.edu.cn

F. Yang

Beijing Percutek Therapeutics Co., Ltd., Beijing 102600, China

X.-Y. Gong

Suzhou Innomed Medical Device Co., Ltd., Suzhou 215123, China

M. Zhao

Schlumberger Technology Corporation, Houston, TX 77054, USA

Y.-F. Zheng, Z.-L. Sun\*

State Key Laboratory for Turbulence and Complex System, College of Engineering, Peking University, Beijing 100871, China

e-mail: sunzhl@pku.edu.cn

Published online: 30 April 2019

**Keywords** Nitinol; Stent-graft system; Abdominal aortic aneurysm; Fatigue safety factor; Radial force; Finite element analysis

#### 1 Introduction

An aortic aneurysm is the enlargement (dilation) of the aorta to greater than 1.5 times the normal size. They usually cause no symptoms except when ruptured. They are most commonly located in the abdominal aorta but can also be located in the thoracic aorta. Aortic aneurysms cause weakness in the wall of the aorta and increase the risk of aortic rupture. When rupture occurs, massive internal bleeding appears and, unless treated immediately, shock and death can occur.

Surgery is the definite treatment of an aortic aneurysm. Medical therapy is typically reserved for smaller aneurysms or for elderly, frail patients where the risks of surgical repair exceed the risks of non-operative therapy (observation alone). Since 1990s, endovascular aneurysm repair (EVAR) has been used in specific cases. In 2003, EVAR surpassed an open aortic surgery as the most common technique for repair of abdominal aortic aneurysm (AAA) [1–4], and in 2010, EVAR accounted for 78% of all intact AAA repair in the United States [5]. Nowadays, EVAR is the most widely used method for the treatment of aortic aneurysm and dissection.

In EVAR, a stent-graft (SG) system crimped into the sheath is guided from the femoral artery to the affected artery segment in order to shield the damaged or diseased parts from the blood circulation. Thus, the primary objective is to exclude the affected artery segment completely from the impact of the pulsatile blood flow. Most of the



stents for EVAR are made of nitinol alloys because of their good biocompatibility [6–8], good resistance to corrosion and fatigue [9–11] and excellent mechanical behaviors [12, 13]. Many works of nitinol stents have been done, some of them based on experimental tests [14–17] while others focused on finite element analysis (FEA) [11, 18–20] or combine FEA with experiments [21, 22].

Numerical study with finite element analysis was performed systematically to each of the stent components in order to design an effective stent-graft system for AAA. Experimental tests were carried out to validate the numerical results. At last, the designed stent-graft system was tested in animal tests and clinical trials.

# 2 Experimental

## 2.1 Preliminary considerations

The self-expanding stent-graft system presented in this work designed for AAA consists of Dacron graft material and nitinol stent components. Three patterns of the stent strut were designed to be used at different locations of the stent-graft system: V-type, W-type and suprarenal. V-type stents are made of one single V-strut as shown in Fig. 1c. W-type stents were made of two kinds of V-struts with the height of 7.5 mm and 5.0 mm alternately, which is shown in Fig. 1d. A suprarenal stent with hooks is shown in Fig. 1b.

For V-type and W-type stents, straight nitinol wires with the diameter of 0.33 mm were winded over a series of fixed pins on a cylindrical surface to form these components. In order to generate the basic structural shape, a heat treatment was applied. A small nitinol tube was used to connect the open ends of each component to make a closed loop.

The nomenclature of the designed stent components is explained here: the name X-Y, where X represents the nominal diameter of the component (the diameter of the cylindrical surface of graft material) and Y represents the height of the V- or W-strut.

For suprarenal stents, the processing method is different from wire stents. Laser cutting was applied on tube nitinol materials to form these components. The height is 15 mm, and the thickness is 0.43 mm. These stent components were then stitched on a smaller cylindrical graft material, as shown in Fig. 1a. Table 1 shows the correspondence among stent, sheath and aorta. Peak number of stent components will increase as the nominal diameter (X) increases to maintain the consistent radial force. Table 2 lists the peak numbers of all the stents.

#### 2.2 FEA method

The stent was crimped into the delivery catheter and then deployed from the catheter to a smaller diameter aorta. After that, cyclical deformation was applied under the blood pressure. The worst-case scenario is assumed as  $\pm$  2.5% radial pulsatile under 100 mmHg blood pressure difference [23]. The introduction of an aorta model will significantly increase the computation amount, and it is obviously inefficient considering the number of stents to be simulated. In order to investigate the fatigue behaviors and radial forces of all the self-expandable nitinol stents, a commercial finite element code ABAQUS 6.13-1 was used to simulate the crimping and self-expansion. Some scripts were written to do the auto post-processing of the open database (ODB) files. The geometry models of Nitinol stents were created by a commercial CAD software SolidWorks 2012.

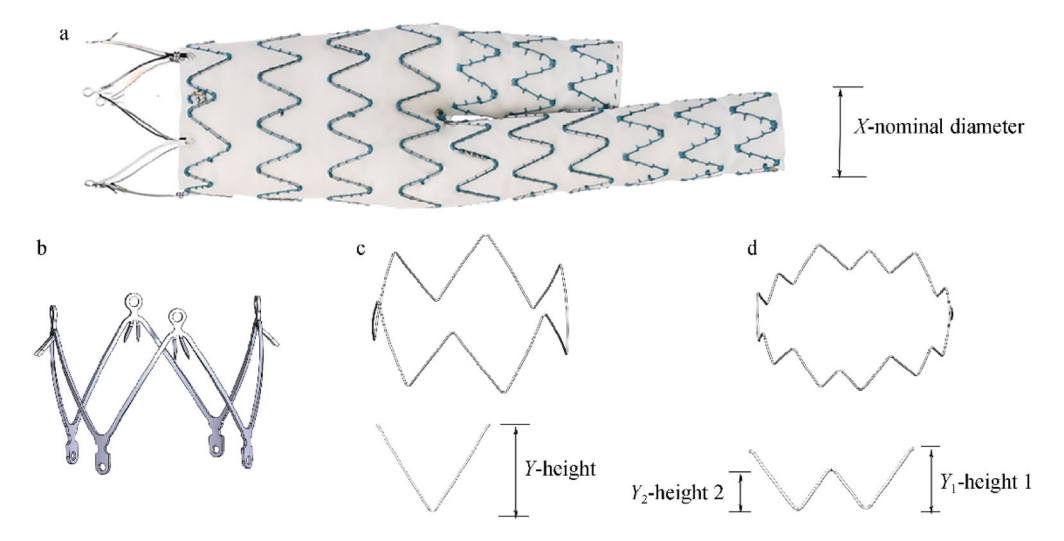


Fig. 1 Stent graft and its components: a full stent graft, b suprarenal stent, c V-type stent and d W-type stent

Table 1 Correspondence among stent, sheath and aorta

Nominal diameter/mm	Inner diameter of sheath/mm	Inner diameter of aorta/mm	Stent graft oversize/%
20	4.8	16	25
22	4.8	18	22
24	5.4	20	20
26	5.4	22	18
28	5.4	24	17
30	6.1	26	15
32	6.1	28	14
34	6.1	30	13
36	6.1	32	13

Table 2 Peak numbers of all stents

Stents	Nominal diameter/mm				
	20, 22	24	26, 28	30, 32, 34, 36	
X-50	10	10	10	12	
X-75	10	10	10	12	
X-150	5	5	5	6	
X-7550	8	10	10	12	
Suprarenal	4	5	5	6	

Only the repetitive section of the stent is analyzed as shown in Fig. 2. Circumferential degree of freedom was fixed at the open ends, and axial degree of freedom of one node was fixed to prevent the rigid body translation. No frictions were applied. A rigid cylinder surface (crimper) was created to control the crimping, self-expanding and pulsatile procedures. For the crimper, both circumferential and axial degrees of freedom were fixed. Two additional rigid surfaces were added to make sure the stent deforms within its original central angle due to self-contact during the first two procedures. For these two rigid surfaces, all degrees of freedom were fixed. The stent was crimped into the sheath at first. Then, it was deployed to the diameter of 1.025*D* (*D*: inner diameter of the aorta). At last, the sent was compressed to the diameter of 0.975*D*.

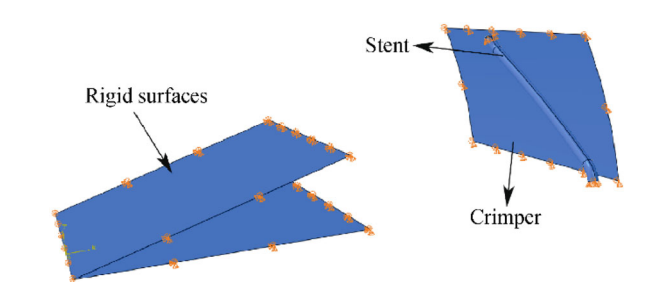


Fig. 2 Boundary conditions

For the stent, the element type is C3D8R (eight-node linear brick, reduced integration). There are 30 nodes along the circumference of the section and 1000 nodes along the axis of the repetitive section of the stent component. For the crimper and the two additional rigid surfaces, there are  $100 \times 100$  SFM3D4R (four-node quadrilateral surface element, reduced integration) elements.

#### 2.3 Materials' properties

Nitinol has a unique superelastic property [24]. A custom user material subroutine was chosen to model the superelastic properties of the material. Parameters of the nitinol material model were provided by Beijing Percutek Therapeutics Co., Ltd.

## 2.4 Experimental tests

After the simulations, the Bose ElectroForce<sup>®</sup> 9150-6 dynamic fatigue testing machine was used to run the fatigue tests. All the stent components went through a 400-million-cycle (10 years *in vivo*) accelerated fatigue test (by improving the frequency to 33 Hz), which took almost 3 months.

#### 2.5 Animal trial

The same sizes of stents for human clinical trials were implanted into 12 sheep with the help of Beijing Anzhen Hospital according to ISO 25539. All the procedures were completed successfully. Six sheep were dissected after 28 days, and the other six sheep were dissected after 180 days.

## 2.6 Clinical trial

All the surgeries were approved by the Ethics Committees of Beijing Anzhen Hospital (2013-035), Chinese PLA

Springer

(People's Liberation Army) General Hospital (2015-015), Shandong Provincial Hospital (2015-02), Zhongshan Hospital (2013-64(2)), the Second Xiangya Hospital of Central South University (2015-15), West China Hospital (2013-15), the First Affiliated Hospital of Sun Yat-sen University (2013-026-02) and the 2nd Affiliated Hospital of Harbin Medical University (2013-030).

A total of 153 AAA patients have participated in clinical trials in eleven hospitals. Among them, 82 patients used present AAA stent-graft systems, while the rest 71 patients used Medtronic Endurant stent-graft systems. All patients were observed for 1 year after operation. Computed tomography (CT) results were carried out by Toshiba CT Aquilion One. The slice increment was 1 mm.

#### 3 Results

#### 3.1 Fatigue safety factor

Fatigue resistance is vital for AAA stent-graft system. Fatigue safety factors can be analyzed using maximum principal strains in the stent [25, 26]. The maximum principal strain at the systolic pressure was defined as  $\varepsilon_1$ , and the one at the diastolic pressure was defined as  $\varepsilon_2$ . We have:

$$\varepsilon_{\text{mean}} = (\varepsilon_1 + \varepsilon_2)/2$$
 (1)

$$\varepsilon_{\text{alt}} = |(\varepsilon_1 - \varepsilon_2)|/2 \tag{2}$$

where  $\varepsilon_{\rm mean}$  and  $\varepsilon_{\rm alt}$  are the mean strain and alternating strain, respectively. Many similar constant-life diagrams have been proposed [27–30]. In this work, a diagram shown in Fig. 3 is used to analyze the stent components' fatigue behaviors.

Fatigue safety factor (FSF) is defined as the ratio of fatigue strain limit ( $\varepsilon_{lim}$ ) and the alternating strain [26]:

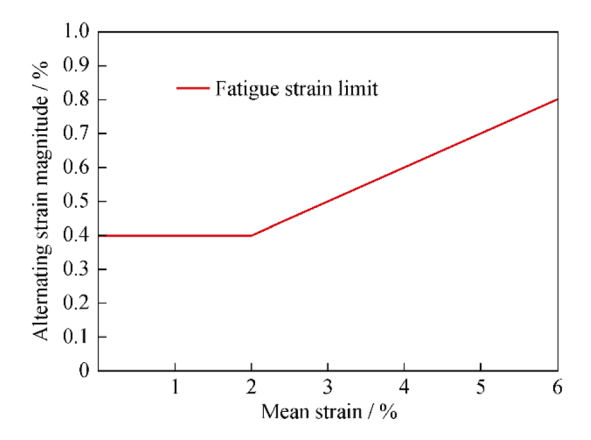


**Fig. 3** Fatigue limit of  $1 \times 10^7$  cycles

$$FSF = \frac{\varepsilon_{lim}}{\varepsilon_{alt}} \tag{3}$$

Figure 4 shows the contours of post-processing results. The contours of the reciprocal of FSFs were plotted. It is obvious that the lowest FSFs occur around the peaks.

All the stent components' FSF are shown in Fig. 5. Theoretically, stents with FSFs above one are considered safe. As a result, all the stent components can provide enough fatigue resistance within  $1 \times 10^7$  cycles.

#### 3.2 Radial force

Figure 6 shows the simplified free body diagram of the stent. CF denotes the contact force between the shell (aorta) and the strut (repetitive section),  $\theta$  represents the strut's corresponding degree of the central angle (Fig. 6), and  $\alpha$  represents the position of CF. For V-type stents,  $\alpha$  equals 0 in the idealized condition because of their high symmetry. For W-type stents,  $\alpha$  is limited but not zero. Based on the theory of thin-walled tubes, the stent geometry can be treated as a hollow cylinder subjected to an internal pressure (P). The relationship between radial force (RF) and hoop force (HF) can be expressed by Eq. (4):

$$RF = 2\pi HF \tag{4}$$

From Fig. 4, the hoop stress at both ends of the repetitive section can be derived as follows:

$$HF_1 = \frac{1}{2}CF \cdot \left(\cos\alpha / \sin\frac{\theta}{2} + \sin\alpha / \cos\frac{\theta}{2}\right)$$
 (5)

$$HF_{2} = \frac{1}{2}CF \cdot \left(\cos \alpha / \sin \frac{\theta}{2} - \sin \alpha / \cos \frac{\theta}{2}\right) \tag{6}$$

When  $\alpha = 0$ ,  $HF_1 = HF_2$ .

Define  $\delta$  as the difference between HF<sub>1</sub> and HF<sub>2</sub>:

$$\delta = HF_1 - HF_2 = CF \cdot \sin \alpha / \cos \frac{\theta}{2}$$
 (7)

Here, the average of HF<sub>1</sub> and HF<sub>2</sub> is defined as the HF:

$$HF = \frac{1}{2}CF \cdot \cos \alpha / \sin \frac{\theta}{2}$$
 (8)

Hence, the radial force (RF) can be calculated as follows:

$$RF = 2\pi HF = \pi \cdot CF \cdot \cos \alpha / \sin \frac{\theta}{2}$$
 (9)

Radial force of all the stent components calculated using the equations above is shown in Fig. 7. For each series, stent components with different nominal diameters tend to provide similar radial forces at a constant level. X-50 series have the largest RFs, while X-150 series have the smallest. The radial force is related to the stiffness of the strut.



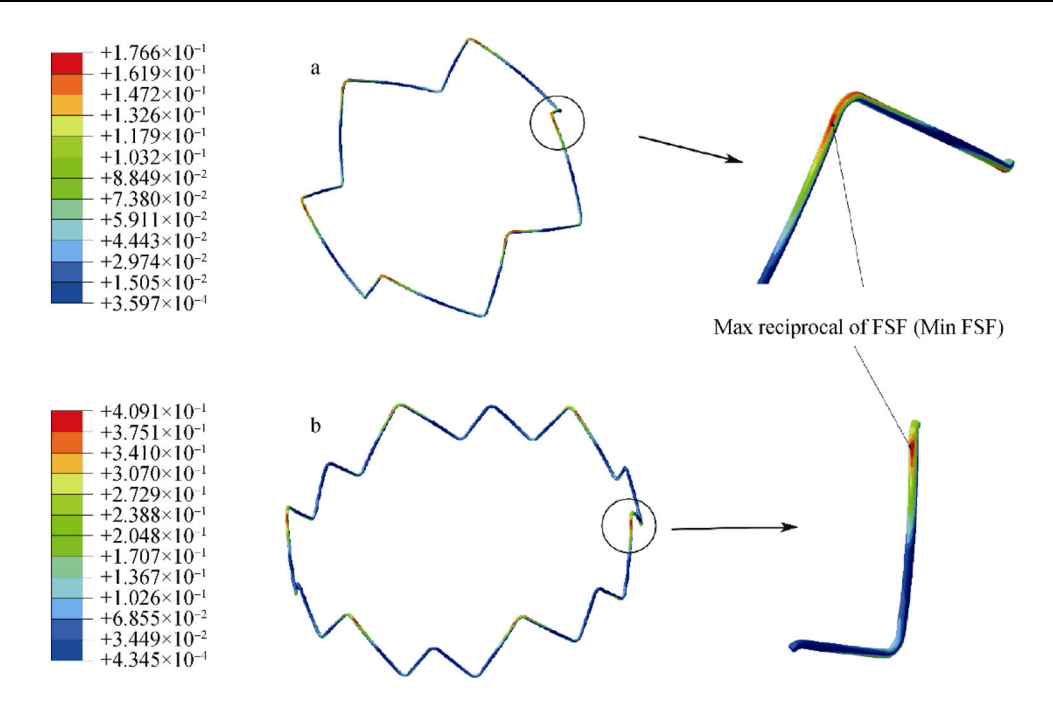


Fig. 4 Reciprocal of FSF contour plot: a V-type stent and b W-type stent

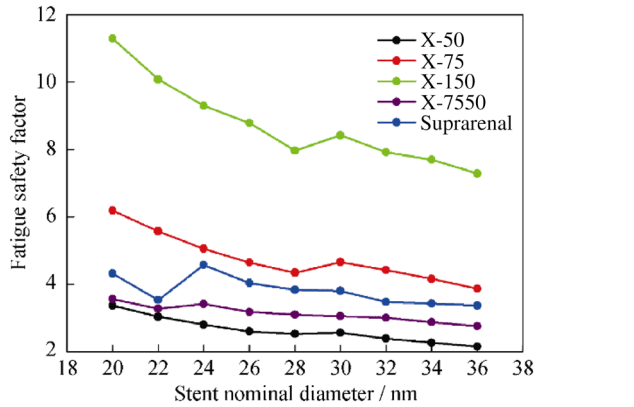


Fig. 5 Fatigue safety factors of each series of stents

 $\label{eq:Stent nominal diameter / nm}$  Fig. 7 Radial forces of each series of stents

22

24

20

6

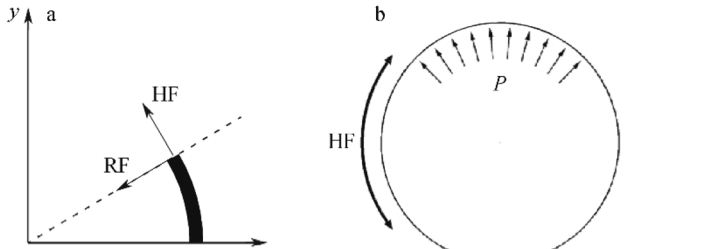
5

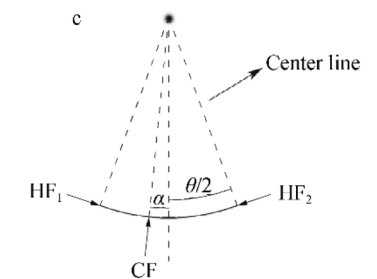
3

2

18

Radial force / N





26 28

X-75 X-150

32

34

30

36 38

Fig. 6 Free body diagram of stent to calculate radial force: a directions of HF and RF, b directions of HF and P and c locations of CF and HF

#### 3.3 Fatigue test

After 400 million cycles, the stents were observed under an optical measuring instrument of 38 times multiplication.

Figure 8 shows structural integrity. No fracture or collapse was observed. Although cracks cannot be found under such low multiplication, they are allowed to exist after 10 years' fatigue.



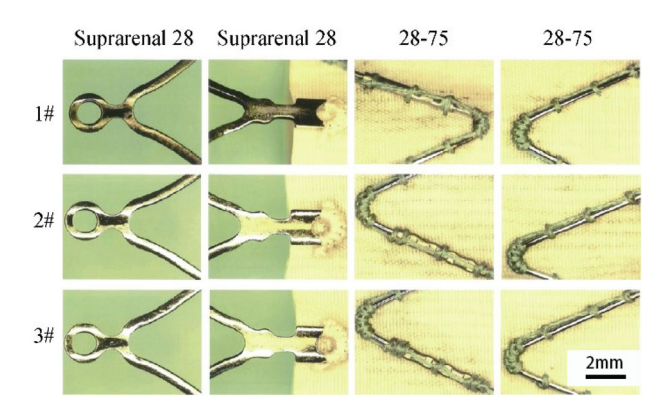


**Fig. 8** Surface topography of three sets of parallel samples under an optical measuring instrument of 38-times multiplication after 400-million-cycle fatigue tests

## 3.4 Animal testing

All the stent-graft systems were well implanted. All the sheep could breathe on their own after the surgeries. No infection occurred. The stent-graft system was tightly bound to the aorta. No lesions took place for the endothelial tissue on the stent. No obvious injury or inflammation was observed. There was no sign of giant cells or granulomas.

## 3.5 Clinical trial

The death rate related to AAA after 365 days is 0% for both Percutek and Medtronic groups. One patient's CT results of blood flow are shown in Fig. 9. The aneurysm was quite obvious before the surgery. After 30-day implantation, the blood flow had been almost controlled within the stent-graft system. There was no obvious difference among the blood flow after 30, 180 and 365 days. The designed stent-graft system has a significant effect.

## 4 Discussion

In order to design an AAA stent-graft system, all the parametric variations of the individual stent components and their effect on the overall stent performance are vital. After a careful selection and arrangement of the individual stent components, an AAA stent-graft system was created (Fig. 10). (1) A suprarenal stent with hooks was used as the first stent at the proximal end to improve the migration resistance, due to the massive blood flow within the abdominal aorta. (2) An AAA stent graft does not require the same level of conformability as TAA (thoracic aortic aneurysm) and TAD (thoracic aortic dissection) because the abdominal aortas do not have natural arches. So, X-50 series stents will not be used because they were difficult to

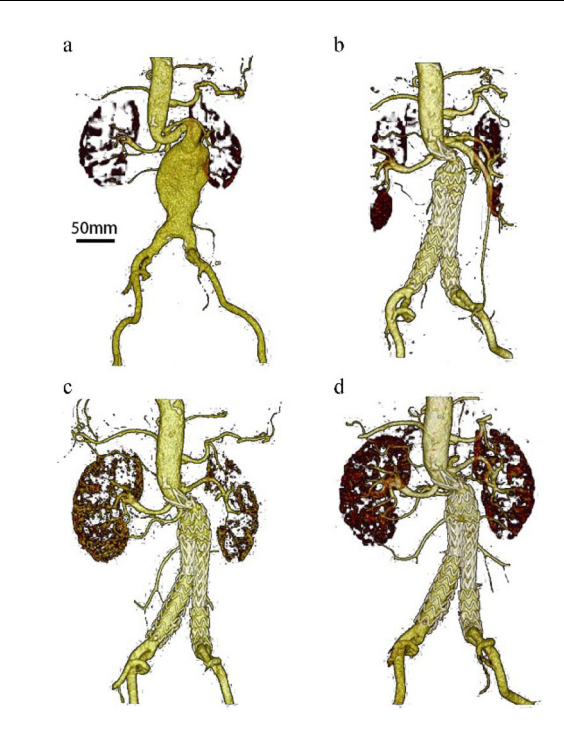


**Fig. 9** Three-dimensional CT blood flow results of a patient's abdominal aorta **a** before surgery and after **b** 30 days, **c** 180 days and **d** 365 days

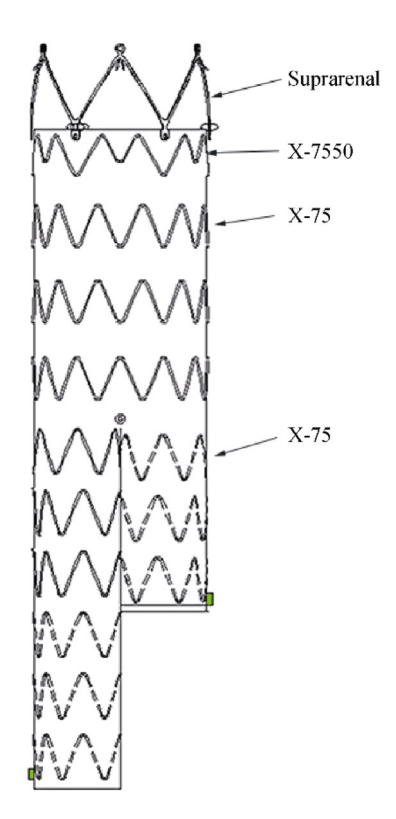


Fig. 10 Stent graft for AAA

crimp and were unstable during the self-expanding process. Sealing is the most important property for AAA. In order to

 $\underline{\underline{\mathscr{D}}}$  Springer

create a perfect seal, the second stent at the proximal end must provide a proper radial force and has enough contact area. X-7550 series have almost the same radial forces with X-75 series while the minimal sealing length can reach 5.0 mm, which is 2.5 mm shorter than that of X-75 series. As a result, an X-7550 stent was chosen as the second stent at the proximal end to seal the graft material and the aorta while also taking safety factors into account. (3) For the middle section and the bifurcations, X-75-0.33 stents were used because their safety factors rank only second to X-150 series while they can also provide good conformability.

The clinical trial has demonstrated very positive results of newly designed stent-graft system. It is comparable with Medtronic Endurant stent-graft systems.

#### 5 Conclusion

Five series of stent components were investigated using FEA methods. Each series of stents have their advantages and disadvantages. Four variables were studied: strut type, strut height, peak number and nominal diameter. Fatigue resistance and radial strength are two of the most important properties of a stent-graft system. After a thoughtful selection and arrangement of the stent components based on FEA results, an AAA-specific stent-graft system was developed.

**Acknowledgements** This work was supported by the National Key Research and Development Program of China (No. 2018YFC1106600).

#### References

- [1] Sethi RKV, Henry AJ, Hevelone ND, Lipsitz SR, Belkin M, Nguyen LL. Impact of hospital market competition on endovascular aneurysm repair adoption and outcomes. J Vasc Surg. 2013;58(3):596.
- [2] Rayt HS, Sutton AJ, London NJM, Sayers RD, Bown MJ. A systematic review and meta-analysis of endovascular repair (EVAR) for ruptured abdominal aortic aneurysm. Eur J Vasc Endovasc Surg. 2008;36(5):536.
- [3] Mastracci TM, Garrido-Olivares L, Cinà Claudio S, Clase CM. Endovascular repair of ruptured abdominal aortic aneurysms: a systematic review and meta-analysis. J Vasc Surg. 2008;47(1): 214.
- [4] Van Beek SC, Conijn AP, Koelemay MJ, Balm R. Editor's choice—endovascular aneurysm repair versus open repair for patients with a ruptured abdominal aortic aneurysm: a systematic review and meta-analysis of short-term survival. Eur J Vasc Endovasc Surg. 2014;47(6):593.
- [5] Dua A, Kuy SR, Lee CJ Jr, Upchurch GR, Desai SS. Epidemiology of aortic aneurysm repair in the United States from 2000 to 2010. J Vasc Surg. 2014;59(6):1512.
- [6] Trépanier C, Leung TK, Tabrizian M, Yahia L, Bienvenu JG, Tanguay JF. Preliminary investigation of the effects of surface

- treatments on biological response to shape memory NiTi stents. J Biomed Mater Res. 1999;48(2):165.
- [7] Thierry B, Merhi Y, Bilodeau L, Trépanier C, Tabrizian M. Nitinol versus stainless steel stents: acute thrombogenicity study in an ex vivo porcine model. Biomaterials. 2002;23(14):2997.
- [8] Ryhänen J, Kallioinen M, Tuukkanen J, Junila J, Niemelä E, Sandvik P. In vivo biocompatibility evaluation of nickel-titanium shape memory metal alloy: muscle and perineural tissue responses and encapsule membrane thickness. J Biomed Mater Res. 2015;41(3):481.
- [9] Duerig TW. Superelastic nitinol for medical devices. Med Plast Biomater. 1997; Article ID 10007700791.
- [10] Schaffer JE, Plumley DL. Fatigue performance of nitinol round wire with varying cold work reductions. J Mater Eng Perform. 2009;18(5–6):563.
- [11] Dordoni E, Meoli A, Wu W, Dubini G, Migliavacca F, Pennati G. Fatigue behaviour of nitinol peripheral stents: the role of plaque shape studied with computational structural analyses. Med Eng Phys. 2014;36(7):842.
- [12] Shabalovskaya SA. On the nature of the biocompatibility and on medical applications of NiTi shape memory and superelastic alloys. Bio-Med Mater Eng. 1996;6(4):267.
- [13] Khamei AA, Dehghani K. A study on the mechanical behavior and microstructural evolution of Ni60 wt%-Ti40 wt% (60Nitinol) intermetallic compound during hot deformation. Mater Chem Phys. 2010;123(1):269.
- [14] James B, Murray S, Saint S. Fracture characterization in nitinol. In: Pelton A, Duerig T, editors. Proceedings of the international conference on shape memory and superelastic technologies (SMST). California: 2003, 321.
- [15] Dyet JF, Watts WG, Ettles DF, Nicholson AA. Mechanical properties of metallic stents: how do these properties influence the choice of stent for specific lesions? Cardiovasc Intervent Radiol. 2000;23(1):47.
- [16] Takuya Tsujimura, Osamu Iida, Masashi Fujita, Masaharu Masuda, Shin Okamoto, Takayuki Ishihara. Two-year clinical outcomes post implantation of Epic<sup>TM</sup> self-expanding nitinol stents for the aortoiliac occlusive disease in patients with peripheral arterial disease. J Atheroscler Thromb. 2018;25(4): 344.
- [17] Laird JR, Zeller T, Loewe C, Chamberlin J, Begg R, Schneider PA. Novel nitinol stent for lesions up to 24 cm in the superficial femoral and proximal popliteal arteries: 24-month results from the TIGRIS randomized trial. J Endovasc Ther. 2018;25(1):68.
- [18] Gao ZY, Liang DK, Qi M, Zhang QB, Yang DZ. The longitudinal flexibility analysis of nitinol self-expanding stent. J Funct Mater. 2007;38(1):113.
- [19] Liang DK, Yang DZ, Qi M. The finite element analysis of superelastic nitinol intravascular stent. J Funct Mater. 2005; 36(3):471.
- [20] Nematzadeh F, Sadrnezhaad SK. Effects of material properties on mechanical performance of nitinol stent designed for femoral artery: finite element analysis. Sci Iran. 2012;19(6):1564.
- [21] Rebelo N, Gong XY, Hall A. Finite element analysis on the cyclic properties of superelastic nitinol. In: Berg B, Mitchell MR, Proft J, editors. Proceedings of the international conference on shape memory and superelastic technologies (SMST), California; 2006. 157.
- [22] Zhao ZX, Liu DZ, Sun K, Luo QY. Finite element analysis and fatigue tests for nitinol vascular stents. Chin J Med Instrum. 2008;32(5):373.
- [23] Duerig T, Pelton A, Stöckel D. An overview of nitinol medical applications. Mater Sci Eng A. 1999;s273–275(99):149.
- [24] Zheng YF, Huang BM, Wang Z. The deformation behavior and mechanism of TiNi alloy exhibiting quasi-linear superelasticity. In: Russell S, Pelton A, editors. Proceedings of the international



- conference on shape memory and superelastic technologies (SMST), California; 2000. 433.
- [25] Kleinstreuer C, Li Z, Basciano CA, Seelecke S, Farber MA. Computational mechanics of nitinol stent grafts. J Biomech. 2008;41(11):2370.
- [26] Pelton AR, Schroeder V, Mitchell MR, Gong XY, Barney M, Robertson SW. Fatigue and durability of nitinol stents. J Mech Behav Biomed Mater. 2008;1(2):153.
- [27] Pelton AR. Nitinol fatigue: a review of microstructures and mechanisms. J Mater Eng Perform. 2011;20(4–5):613.
- [28] Early M, Kelly DJ. The consequences of the mechanical environment of peripheral arteries for nitinol stenting. Med Biol Eng Comput. 2011;49(11):1279.
- [29] Holtz RL, Sadananda K, Imam MA. Fatigue thresholds of Ni-Ti alloy near the shape memory transition temperature. Int J Fatigue. 1999;21(S1):137.
- [30] Jr MN, Brookes PC, Cory JS. NiTi fatigue behavior. J Appl Phys. 1981;52(12):7442.

